WILEY-VCH

DOI: 10.1002/((please add manuscript number))
Article type: Full Paper

Photon Upconverting Solid Films with Improved Efficiency for Endowing Near-Infrared Sensitivity to Perovskite Solar Cells

Mika Kinoshita, Yoichi Sasaki, Shogo Amemori, Naoyuki Harada, Zhanhao Hu, Zonghao Liu, Luis K. Ono, Yabing Qi, Nobuhiro Yanai,* and Nobuo Kimizuka**

M. Kinoshita, Y. Sasaki, N. Harada, Prof. N. Yanai, Prof. N. Kimizuka
Department of Chemistry and Biochemistry, Faculty of Engineering, Center for Molecular Systems (CMS), Kyushu University, Moto-oka 744, Nishi-ku, Fukuoka 819-0395, Japan
E-mail: yanai@mail.cstm.kyushu-u.ac.jp
n-kimi@mail.cstm.kyushu-u.ac.jp
Prof. S. Amemori
Institute for Frontier Science Initiative, Kanazawa University, Kakuma-machi, Kanazawa 920-1192, Japan
Dr. Z. Hu, Dr. Z. Liu, Dr. L. K. Ono, Prof. Y. B. Qi
Energy Materials and Surface Sciences Unit (EMSSU), Okinawa Institute of Science and Technology Graduate University (OIST), 1919-1 Tancha, Kunigami-gun, Onna-son, Okinawa 904-0495, Japan
E-mail: Yabing.Qi@OIST.jp
Prof. N. Yanai
PRESTO, JST, Honcho 4-1-8, Kawaguchi, Saitama 332-0012, Japan

Keywords: photon upconversion, triplet-triplet annihilation, energy collection, perovskite, solar cell

Abstract:

Perovskite solar cells have emerged as the next-generation high-efficiency solar cell, but their absorption is mostly limited to the visible (vis) range. One possible solution is to integrate near-infrared (NIR)-to-vis photon upconversion (UC). Herein, we show the first example of endowing NIR sensitivity to the perovskite solar cells by using solid films showing the NIR-to-vis UC based on triplet-triplet annihilation (TTA). High TTA-UC efficiency of 4.1±0.3% at an excitation intensity of 125 W/cm^2 is achieved by sensitizing rubrene (acceptor) triplet with osmium (Os) complex donor having singlet-to-triplet (S-T) absorption in the NIR range, and by increasing the fluorescence quantum yield through energy harvesting to a highly fluorescent collector. In particular, our spectroscopic studies indicate that the upconverted acceptor singlet energy is almost selectively transferred to the collector rather than being quenched by the donor. By attaching the TTA-UC film behind a semi-transparent perovskite solar cell, a photocurrent generation is observed under the excitation at 938 nm.

1. Introduction

Photon upconversion (UC) enables the conversion of lower-energy light into higher-energy light. Effective utilization of the unused near-infrared (NIR) photons by NIR-to-visible (vis) UC is anticipated because it has the potential to overcome the Shockley−Queisser limit as recently demonstrated for various solar cells.[1-4] The NIR-to-vis UC is particularly critical to the recently-emerged lead halide-based perovskite solar cells whose absorption is mostly limited to the wavelength range below 800 nm.[5, 6] There have been reports on

the integration of lanthanide-based NIR-to-vis upconversion nanoparticles into perovskite solar cells, but the effective utilization of NIR light at the solar irradiance remains challenging.[7-10] As an alternative UC mechanism, triplet-triplet annihilation-based photon upconversion (TTA-UC) has attracted much attention for solar energy applications because it works with low-intensity light such as sunlight.[11-22] In the typical mechanism of TTA-UC, an excited triplet state of emitter (acceptor) molecules is populated by triplet energy transfer (TET) from sensitizer (donor) molecules with high intersystem crossing (ISC) efficiency. This is followed by annihilation between two emitter triplets, and the resulting higher-energy emitter excited singlet emits the upconverted delayed fluorescence.

However, this mechanism faced a problem in upconverting NIR light that arises from the large energy loss (hundreds of meV) during the ISC of the donors. This issue has been overcome by employing new-generation triplet sensitizers. Much less or no energy loss in the ISC process was attained for semiconductor nanocrystals and osmium (Os) complexes with singlet-to-triplet (S-T) absorption.[23-31] Meanwhile, solid-state upconverters are desirable for device applications. The groups of Bulović, Bawendi, and Baldo achieved the NIR-to-vis TTA-UC in the solid-state.[21, 30] They vacuum-deposited acceptor rubrene and emitter dibenzotetraphenylperiflanthene (DBP) on a PbS nanocrystal monolayer, in which photoexcited energy was effectively transferred from PbS to rubrene, and the upconverted singlet energy was harvested from rubrene to DBP. Kazlauskas et al. have also reported the increase of TTA-UC efficiency by the addition of DBP into spin-coated films of rubrene and *t*-butyl-substituted rubrene.[32] Our group reported the NIR-to-vis TTA-UC by employing the Os complex $Os(atpy)(tbbpy)Cl^+$ (atpy = tris(2-ethylhexyl)-[2,2':6',2''-terpyridine]-4,4',4''-

tricarboxamide; tbbpy = 4,4'-di-*tert*-butyl-2,2'-bipyridine) that shows the S-T absorption over 900 nm.[28] The Os complex was molecularly doped in amorphous nanoparticles of rubrene by the simple aqueous reprecipitation method. The obtained nanoparticles were further dispersed in poly(vinyl alcohol) (PVA) to avoid the oxygen quenching of the triplet states. All the processes were carried out in air, and no further complicated sealing processes were necessary to achieve the in-air NIR-to-vis TTA-UC.

Here, we combine the approaches using the S-T absorption donor and the highly fluorescent singlet energy collector DBP to improve the TTA-UC efficiency (Figure 1b). As expected, the addition of the singlet energy collector increases the fluorescence quantum yield by outcompeting with other deactivation processes such as singlet fission.[21, 30, 33] Thanks to the spatial separation between the collector and the donor in the acceptor nanoparticles, the singlet back energy transfer from the collector to the donor is largely suppressed. [34] Interestingly, we also demonstrate a highly selective Förster resonance energy transfer (FRET) from acceptor to collector rather than donor (Figure 1b). The integration of the NIR-to-vis TTA-UC films on the back of the perovskite cells leads to photocurrent generation under NIR light excitation (938 nm, Figure 1a).

2. Results and Discussion

2.1. Preparation of TTA-UC films

Rubrene nanoparticles doped with the S-T absorption donor Os(atpy)(tbbpy)Cl^+ and the singlet energy collector DBP were prepared by the reprecipitation method (Figure 2a).[28] A 1.5 mL THF solution containing Os(atpy)(tbbpy)Cl^+ (0.02 mM), rubrene (5 mM) and DBP (varied concentrations, 0.0025−0.15 mM) was

rapidly injected into 7.5 mL of aqueous sodium dodecyl sulfate (SDS, 10 mM), and the formed solid particles were collected by centrifugation. For the preparation of ternary films, an optimized molar ratio of Os(atpy)(tbbpy)Cl^+:rubrene:DBP = 0.4:100:0.5 was used. Dynamic light scattering (DLS) measurements of Os(atpy)(tbbpy)Cl^+/rubrene/DBP particles showed an average particle size of 255 nm (Figure 2b). Scanning electron microscopy (SEM) showed spherical structures with an average diameter of ca. 200 nm (Figure 2c), which is in good agreement with the DLS result. The ζ-potential of the particles was determined as −58 mV, indicating the surface coverage of nanoparticles with anionic SDS. The X-ray powder diffraction (XRPD) pattern of the nanoparticles did not show any sharp peaks, indicating the amorphous structure (Figure S1). Os(atpy)(tbbpy)Cl^+/rubrene/DBP nanoparticles have almost the same shape characteristic as Os(atpy)(tbbpy)Cl^+/rubrene nanoparticles in our previous report.[28] The nanoparticles were re-dispersed in an aqueous solution of PVA (15 wt%), which was cast on a glass plate and dried under vacuum to form a highly transparent film. PVA works as the oxygen blocking matrix to protect the excited triplets.[28] PVA films containing rubrene nanoparticles and binary rubrene/DBP nanoparticles were also prepared for spectral characterizations.

2.2. Characterizations of TTA-UC properties

Under excitation with a 938 nm NIR laser, an upconverted emission was observed in the vis range from the Os(atpy)(tbbpy)Cl^+/rubrene/DBP ternary film (Figure 3a), which showed different emission peak position (625 nm) from the Os(atpy)(tbbpy)Cl^+/rubrene binary film (575 nm) (Figure 3b). The difference in the spectral

shape of upconverted emission between these two samples reflects the collection of upconverted singlet energy to DBP. The absolute TTA-UC efficiency was obtained by exciting the films in the integrating sphere in air. Note that the quantum yield is generally defined as the ratio of emitted photon numbers to absorbed photon numbers, and thus the theoretical maximum of the TTA-UC quantum yield (Φ_{UC}) is 50%. Meanwhile, in many reports, this value is multiplied by 2 to set the maximum conversion efficiency at 100%. To avoid confusion arising from the different definitions, the UC efficiency is written as Φ_{UC}' (= $2\Phi_{UC}$) when the maximum value is standardized to 100%. The Os(atpy)(tbbpy)Cl^+/rubrene binary film showed the Φ_{UC}' value of 0.43% at around 150 W/cm^2, in which the 730 nm laser was used as the excitation source due to the insufficient sensitivity of the detector at 938 nm.[28] A much higher NIR-to-vis TTA-UC efficiency of Φ_{UC}' = 4.1 ± 0.3% was observed from the Os(atpy)(tbbpy)Cl^+/rubrene/DBP ternary film at 125 W/cm^2. This obtained value is comparable to the best NIR-to-vis TTA-UC solid systems,[21, 30] and further improvement would be expected by increasing the statistical probability to obtain a singlet from two triplets through the control of higher triplet energy levels.[35,36]

Generally, TTA-UC emission intensity shows a quadratic-to-linear transition with increasing excitation intensity, and the transition point gives a threshold excitation intensity (I_{th}).[37-39] Above I_{th}, TTA becomes the main deactivation channel for the acceptor triplets. Both of the binary Os(atpy)(tbbpy)Cl^+/rubrene film and the ternary Os(atpy)(tbbpy)Cl^+/rubrene/DBP film showed the quadratic-to-linear transition and similar I_{th} values of around 10 W/cm^2 (Figure 3c). Besides, both of the binary and ternary films showed similar UC emission decay curves with an identical triplet lifetime τ_T of 48 μs (Figure 3d). The observed similar I_{th} and

τ_T values indicate that the TTA process takes place only between acceptor rubrene molecules, in which the collector DBP molecules are not involved, as discussed previously.[21] This is reasonable since calculations indicate that the triplet energy level of DBP is ca. 0.2 eV higher than that of rubrene.[40]

2.3. Understanding of the improved TTA-UC efficiency

The FRET process from the acceptor to the collector was characterized by fluorescence quantum yield, lifetime, and spectra of collector-doped acceptor (rubrene/DBP) films in the absence of donor. The fluorescence quantum yield Φ_{FL} increased with the increase of the collector ratio and reached 84% at 0.5 mol% of the collector (Figure 4a). This result indicates that the acceptor-to-collector FRET process outcompetes with the other deactivation processes, such as singlet fission.[21,32] The occurrence of FRET is also confirmed by the shortening of acceptor fluorescence decay (Figure S2). The shape of fluorescence spectra changed with the increase in the collector ratio, and the original rubrene fluorescence mostly disappeared and the DBP fluorescence dominated at 0.5 mol% of collector DBP (Figure 4b). The further increase of the collector ratio up to 3 mol% lead to a redshift and broadening of the fluorescence spectra, suggesting the partial aggregation of DBP molecules. The aggregation of collector DBP is also reflected in the decrease of the Φ_{FL} value at 3 mol% DBP.

In addition to the enhanced fluorescence quantum yield, we found that the addition of collector DBP reduces the back energy transfer to the donor molecules.[32,34] The back energy transfer efficiency Φ_{BET} was estimated from the following equation, $\phi_{BET} = 1 - \tau/\tau_0$, where τ and τ_0 represent the fluorescence lifetime with/without

the donor, respectively. The decay of Os(atpy)(tbbpy)Cl^+/rubrene film became faster than that of rubrene film, indicating the presence of severe acceptor-to-donor back energy transfer (Figure 4c). The average fluorescence lifetime decreased from 16.5 to 6.0 ns, giving a Φ_{BET} value of 64%. This large back energy transfer limits the final TTA-UC efficiency. In stark contrast, the fluorescence decay of the collector was much less sensitive to the addition of donor Os(atpy)(tbbpy)Cl^+ (Figure 4d). The average fluorescence lifetime showed a small decrease from 7.5 ns (rubrene/DBP film) to 5.7 ns (Os(atpy)(tbbpy)Cl^+/rubrene/DBP film) by adding the donor. The Φ_{BET} value of the ternary system was 24%, which is much smaller than the binary system (64%). Although there is a spectral overlap between collector fluorescence and donor absorption, the spatial separation between collector and donor in the acceptor nanoparticles should be responsible for the observed suppression of the back energy transfer. Compared with the previous binary film (Os(atpy)(tbbpy)Cl^+/rubrene film), the current ternary Os(atpy)(tbbpy)Cl^+/rubrene/DBP film has 5-6 times higher Φ_{FL} and about 2 times higher 1- Φ_{BET} value. These differences reasonably explain the ca. 10 times higher UC efficiency of the ternary film as compared with that of the binary film.

Interestingly, we found the highly selective acceptor-to-collector singlet energy harvesting rather than the acceptor-to-donor back energy transfer by measuring the fluorescence quantum yield Φ_{FL} of the Os(atpy)(tbbpy)Cl^+/rubrene/DBP ternary film. The ternary film was excited at two different excitation wavelengths, 462 nm and 598 nm, to selectively excite the acceptor and the collector, respectively (Figure S3). In both cases, the final fluorescence comes from the collector DBP. Interestingly, both cases showed the same Φ_{FL} value of 25%, indicating that the singlet excited energy formed in rubrene is selectively transferred

to the collector rather than being quenched by the donor. Note that the Φ_{FL} value is underestimated than the intrinsic film property due to the reabsorption of fluorescence by the donor in the integrating sphere. For the same reason, the absolute TTA-UC efficiency Φ_{UC}' of the film samples is inevitably underestimated, but it is difficult to precisely correct the contribution of reabsorption since the donor phosphorescence, necessary for the reabsorption calibration,[41] was too weak to detect.

The selective collection of singlet excited energy can be achieved by a larger FRET rate constant from rubrene to DBP than that to Os(atpy)(tbbpy)Cl^+. The FRET rate constant from rubrene to DBP or Os(atpy)(tbbpy)Cl^+ at distance R can be described as follows,[42]

$$k = \frac{1}{\tau}\left(\frac{R_0}{R}\right)^6 \quad , R_0 = 0.2108\left[\kappa^2 {\Phi_D}^0 n^{-4} \int_0^\infty I_D(\lambda)\varepsilon_A(\lambda)\lambda^4 \, d\lambda\right]^{\frac{1}{6}}$$

where τ is the fluorescence lifetime of rubrene in the absence of donor and collector, κ^2 is an orientation factor, $\Phi_D{}^0$ is the fluorescence quantum yield of rubrene, and n is the refractive index. The integral is called the spectral overlap integral and is often denoted as J. I_D is the normalized fluorescence spectrum of rubrene, ε_A is the molar absorptivity (M^{-1} cm^{-1}) of DBP or Os(atpy)(tbbpy)Cl^+, and λ is the wavelength (nm). Considering the similar concentration of Os(atpy)(tbbpy)Cl^+ (0.4 mol%) and DBP (0.5 mol%) in rubrene nanoparticles, R value can be assumed to be similar. In amorphous rubrene nanoparticles, the orientation of donor and collector can be assumed to be random. Hence, the difference in FRET rate constant k mainly depends on the J values. Based on experimental J values, the k value of rubrene-to-DBP FRET is about 8 times larger than that of

rubrene-to-Os(atpy)(tbbpy)Cl^+ FRET (Figure 4e). Therefore, the selective singlet energy harvesting from acceptor to collector against donor is explained by the larger spectral overlap.

2.4. Integration of NIR-to-vis TTA-UC on the perovskite solar cell

The application of NIR-to-vis TTA-UC is demonstrated in the photocurrent generation of semi-transparent perovskite solar cells. As shown in Figure S4, an employed perovskite ($Cs_{0.05}FA_{0.54}MA_{0.41}Pb(I_{0.98}Br_{0.02})_3$) does not show absorption above 800 nm, but the upconverted light (600 ~ 800 nm) of the TTA-UC film is within the absorption range of the perovskite. To integrate the TTA-UC film with the solar cell, TTA-UC film was drop-casted on the Ag substrate which functions as a reflector. The TTA-UC stack was simply attached on the back electrode of the solar cell device (Figure S5), so that the solar cell can receive the upconverted visible light (Figure 5a). While no short-circuit photocurrent was observed in the absence of the UC film under the NIR (938 nm) excitation, the addition of the UC film significantly enhanced the photocurrent (Figure 5b). Double-logarithmic plots of the photocurrent density as a function of excitation intensity at 938 nm showed a transition from quadratic to linear dependence. The transition intensity of 20 W/cm^2 was slightly higher than I_{th} = 10 W/cm^2 for the excitation intensity dependence of UC emission intensity. This is reasonable by taking account that ca. 16% of the excitation light transmitted the solar cell (Figure S6) and the effective excitation intensity is increased by the mirror. These results show the first demonstration of photocurrent generation of perovskite solar cells by the NIR-to-vis TTA-UC emission.

3. Conclusion

In conclusion, we report the improved NIR-to-vis TTA-UC efficiency of solid films by combining the two strategies, the S-T absorption and the singlet energy collection. The use of the S-T absorption donor allows effective triplet sensitization under the NIR excitation since it eliminates the energy loss due to ISC. The introduction of the singlet energy collector allows the improvement of fluorescence quantum yield and the suppression of back energy transfer. In addition, we found that the upconverted acceptor singlet energy is harvested to the collector with a good selectivity rather than quenched by the donor, which can be explained by the larger FRET rate constant. The photocurrent generation of perovskite solar cells by NIR-to-vis TTA-UC is demonstrated for the first time. While further efforts are needed to reduce the excitation intensity to 1 sun by developing new upconversion materials and device structures, this work provides an important step towards achieving higher photovoltaic efficiencies beyond the Shockley-Quiesser limit by the NIR-to-vis TTA-UC.

4. Experimental Section

Sample preparation

All solvents were used as received without further purification. The synthesis and characterization of donor $Os(atpy)(tbbpy)Cl^+$ were reported in our previous work.[28] 5,6,11,12-Tetraphenylnaphthacene (rubrene, purified by sublimation) was purchased from TCI and used as received. Dibenzotetraphenylperiflanthene (DBP, purified by HPLC) was purchased from Aldrich and used as received. For preparation of UC samples,

rubrene (5 mM), Os(atpy)(tbbpy)Cl^+ (0.02 mM), and DBP (0.025 mM) in THF (1.5 mL) was rapidly injected into 7.5 mL of 10 mM sodium dodecyl sulfate (SDS, Nacalai tesque) aqueous solution. After 8 hours of standing at 25 ℃, the precipitate was separated and purified by centrifugation at 10,000 rpm for two times. The precipitate was added to 15 wt% aqueous solution of poly(vinyl alcohol) (PVA, M_w = 31,000-50,000, Aldrich). The suspension was cast on glass plates and dried under vacuum to form nanoparticle-embedded PVA films.

Fabrication of the solar cells

All reagents were used as received without further purification, including PbI_2 (99.99%, TCI), formamidinium iodide (FAI, greatcell solar), methylammonium iodide (MAI, greatcell solar), methylammonium bromide (MABr, greatcell solar), methylammonium chloride (MACl, greatcell solar), cesium iodide (Sigma-Aldrich), 4-*tert*-butylpyridine (99.9%, Sigma Aldrich), acetonitrile (99.9%, Sigma-Aldrich), chlorobenzene (99.8%, Wako), 2,2',7,7'-tetrakis(*N,N*-di-p-methoxyphenylamine)-9,9'-spirobifluorene (spiro-OMeTAD, Merck), SnO_2 (Alfa Aesar, tin(IV) oxide, 15% in H_2O colloidal dispersion), isopropanol (Wako), *N,N*-dimethylformamide (DMF, Wako), dimethyl sulfoxide (DMSO, Wako).

The ITO substrate was sequentially washed with distilled water, acetone, ethanol and isopropanol, and then treated with UV/O_3 for 30 min. The SnO_2 layer was subsequently coated on the ITO substrate with a SnO_2 nanocrystal solution (diluted by H_2O to 2.5%) at 3000 rpm for 30 s, and annealed at 150 °C for 30 min in air. Then, a 1.35 M PbI_2 and 0.0675 M CsI solution (dissolved in mixed DMF/DMSO (V:V = 19:1) solvent and stirred at 70 °C for 2 hours before filtered with PTFE syringe filters) was spin-coated on the substrate at 2000

rpm for 30 s. Then a mixed organic cation solution (FAI 400 mg; MAI 200 mg; MABr 50 mg; MACl 50 mg, dissolved in 10 mL isopropanol) was spin-coated at 1750 rpm for 30 s and then annealed at 150 °C for 15 min in air. Then the hole transport material (HTM) solution was deposited by spin coating at 3000 rpm for 30 s. The spiro-OMeTAD solution was prepared by dissolving spiro-OMeTAD in chlorobenzene (72.3 mg mL^{-1}) with the addition of 17.5 μL Li-TFSI/acetonitrile (520 mg mL^{-1}), and 28.8 μL 4-*tert*-butylpyridine. As a semi-transparent electrode, a gold layer with a thickness of 15 nm followed by 20 nm MoO_3 was deposited through a shadow mask via thermal evaporation in vacuum (10^{-5} Torr).

Device structure

Solar cell structure is indium tin oxide (ITO)/SnO_2 (solution-processed)/$Cs_{0.05}FA_{0.54}MA_{0.41}Pb(I_{0.98}Br_{0.02})_3$/spiro-OMeTAD/Au (15 nm)/MoO_3 (20 nm), where Au/MoO_3 functions as the transparent electrode.[43, 44] From the transmission spectrum of the solar cell device in Figure S6, about 16% of the 938 nm light transmits the device to reach the TTA-UC layer. The upconverted emission (500 ~ 700 nm) is reflected back to the perovskite layer for photocurrent generation. For devices integrated with the TTA-UC, the TTA-UC material was drop-casted on a silver layer (100 nm, functions as a reflector) deposited on a glass substrate. It is then simply capped on the solar cell rear side to form the integrated device as shown in Figure S5.

Measurements

To record TTA-UC emission spectra, a diode laser (938 nm, 90 mW, RGB photonics) was used as an excitation source. The laser power was controlled by combining a software (Ltune) and a variable neutral

density filter and measured using a PD300-UV photodiode sensor (OPHIR Photonics). The laser beam was focused on a sample using a lens. The diameter of the laser beam ($1/e^2$) was measured at the sample position using a CCD beam profiler SP620 (OPHIR Photonics). The emitted light was collimated by an achromatic lens, the excitation light was removed using a short-pass filter (810 nm), and the emitted light was again focused by an achromatic lens to an optical fiber connected to a multichannel detector MCPD-9800 (Otsuka Electronics).

TTA-UC efficiency was measured by using an absolute quantum yield measurement system C13534-01 (Hamamatsu Photonics).[41] The sample was held in an integrating sphere and excited by the laser excitation source (730 nm, 25 mW, RGB photonics). The scattered excitation light was removed using a 700 nm short-pass filter, and emitted light was monitored with a multichannel detector. The spectrometer was calibrated including the integration sphere and short-pass filter by Hamamatsu Photonics. The calibration of the absolute quantum yield measurement system was confirmed by measuring the fluorescence quantum yield of indocyanine green in DMSO under excitation at 730 nm using the laser excitation source. An observed fluorescence quantum yield of 13% was similar to the literature value (12%).[45] The calibration including the short-pass filter was confirmed by observing similar absolute UC quantum yields of palladium(II) octabutoxyphthalocyanine (20 μM)−rubrene (10 mM) in deaerated THF with (0.36%) and without (0.34%) the short-pass filter at an excitation intensity of 24 mW cm^{-2}.

Absorption spectra were recorded on a JASCO V-670 spectrophotometer. Fluorescence spectra were measured by using a PerkinElmer LS 55 fluorescence spectrometer and a JASCO FP-8700 NIR

Spectrofluorometer. Fluorescence quantum yields were measured by using a Hamamatsu Photonics C9920-02 instrument. Time-resolved fluorescence lifetime measurements were carried out by using a time-correlated single-photon counting lifetime spectroscopy system, HAMAMATSU Quantaurus-Tau C11367-02. UC lifetimes were measured by using a UNISOKU TSP-2000. Dynamic light scattering (DLS) and zeta potential measurements were performed on a Malvern Zeta sizer Nanoseries instrument. Scanning electron microscopy (SEM) images were obtained using the Hitachi UHR FE-SEM SU9000 system. Short-circuit current of perovskite solar cells was measured by using a Source Meter, KEITHLEY 2401. The absorbance of the perovskite and transmission of the solar cell device was acquired using a UV-Vis spectrometer JASCO V-670.

Supporting Information

Supporting Information is available from the Wiley Online Library or from the author.

Acknowledgments

This work was partly supported by JSPS KAKENHI grant number JP20H02713, JP17H04799, JP16H06513, the Yoshida Foundation for the Promotion of Learning and Education, the Sumitomo Foundation, the Ogasawara Foundation, and the “Innovation inspired by Nature” Research Support Program, Sekisui Chemical Co. Ltd. The work performed at OIST was supported by funding from the Energy Materials and Surface Sciences Unit of the Okinawa Institute of Science and Technology Graduate University, the OIST R&D Cluster Research Program, the OIST Proof of Concept (POC) Program, and JSPS KAKENHI Grant Number JP18K05266.

Received: ((will be filled in by the editorial staff))
Revised: ((will be filled in by the editorial staff))
Published online: ((will be filled in by the editorial staff))

References

[1] W. Shockley, H. J. Queisser, *J. Appl. Phys.* **1961**, *32*, 510.
[2] T. Trupke, M. A. Green, P. Würfel, *J. Appl. Phys.* **2002**, *92*, 1668.
[3] T. F. Schulze, T. W. Schmidt, *Energy Environ. Sci.* **2015**, *8*, 103.
[4] T. Dilbeck, K. Hanson, *J. Phys. Chem. Lett.* **2018**, *9*, 5810.
[5] A. Kojima, K. Teshima, Y. Shirai, T. Miyasaka, *J. Am. Chem. Soc.* **2009**, *131*, 6050.
[6] M. A. Green, A. Ho-Baillie, H. J. Snaith, *Nat. Photon.* **2014**, *8*, 506.
[7] M. He, X. Pang, X. Liu, B. Jiang, Y. He, H. Snaith, Z. Lin, *Angew. Chem.* **2016**, *55*, 4280.
[8] M. Que, W. Que, X. Yin, P. Chen, Y. Yang, J. Hu, B. Yub, Y. Du, *Nanoscale*, **2016**, *8*, 14432.
[9] F.-L. Meng, J.-J. Wu, E.-F. Zhao,.Y.-Z. Zheng, M.-L. Huang, L.-M. Dai, X. Tao, J.-F. Chen, *Nanoscale*, **2017**, *9*, 18535.
[10] H. Li, C. Chen, J. Jin, W. Bi, B. Zhang, X. Chen, L. Xu, D. Liu, Q. Dai, H. Song, *Nano Energy*, **2018**, *50*, 699.
[11] S. Baluschev, T. Miteva, V. Yakutkin, G. Nelles, A. Yasuda, G. Wegner, *Phys. Rev. Lett.* **2006**, *97*, 143903.
[12] T. N. Singh-Rachford, F. N. Castellano, *Coord. Chem. Rev.* **2010**, *254*, 2560.
[13] J. Zhao, S. Ji, H. Guo, *RSC Adv.* **2011**, *1*, 937.
[14] J.-H. Kim, J.-H. Kim, *J. Am. Chem. Soc.* **2012**, *134*, 17478.
[15] A. Monguzzi, R. Tubino, S. Hoseinkhani, M. Campione, F. Meinardi, *Phys. Chem. Chem. Phys.* **2012**, *14*, 4322.
[16] Y. C. Simon, C. Weder, *J. Mater. Chem.* **2012**, *22*, 20817.
[17] K. Börjesson, D. Dzebo, B. Albinsson, K. Moth-Poulsen, *J. Mater. Chem. A* **2013**, *1,* 8521.
[18] J. Zhou, Q. Liu, W. Feng, Y. Sun, F. Li, *Chem. Rev.* **2015**, *115*, 395.
[19] R. Andernach, H. Utzat, S. D. Dimitrov, I. McCulloch, M. Heeney, J. R. Durrant, H. Bronstein, *J. Am. Chem. Soc.* **2015**, *137*, 10383.
[20] N. Yanai, N. Kimizuka, *Chem. Commun.* **2016**, *52*, 5354.
[21] S. P. Hill, K. Hanson, *J. Am. Chem. Soc.* **2017**, *139*, 10988.
[22] Z. Huang, M. L. Tang, *J. Am. Chem. Soc.* **2017**, *139*, 9412.
[23] Z. Huang, X. Li, M. Mahboub, K. M. Hanson, V. M. Nichols, H. Le, M. L. Tang, C. J. Bardeen, *Nano Lett.* **2015**, *15*, 5552.
[24] C. Mongin, S. Garakyaraghi, N. Razgoniaeva, M. Zamkov, F. N. Castellano, *Science* **2016**, *351*, 369.

[25] M. Wu, D. N. Congreve, M. W. B. Wilson, J. Jean, N. Geva, M. Welborn, T. V. Voorhis, V. Bulović, M. G. Bawendi, M. A. Baldo, *Nat. Photon.* **2016**, *10*, 31.

[26] N. Yanai, N. Kimizuka, *Acc. Chem. Res.* **2017**, *50*, 2487.

[27] N. Nishimura, J. R. Allardice, J. Xiao, Q. Gu, V. Gray, A. Rao, *Chem. Sci.* **2019**, *10*, 4750.

[28] S. Amemori, Y. Sasaki, N. Yanai, N. Kimizuka, *J. Am. Chem. Soc.* **2016**, *138*, 8702.

[29] Y. Sasaki, S. Amemori, H. Kouno, N. Yanai, N. Kimizuka, *J. Mater. Chem. C* **2017**, *5*, 5063.

[30] L. Nienhaus, M. Wu, N. Geva, J. J. Shepherd, M. W. B. Wilson, V. Bulović, T. Van Voorhis, M. A. Baldo, M. G. Bawendi, *ACS Nano* **2017**, *11*, 7848.

[31] Z. Huang, Z. Xu, M. Mahboub, Z. Liang, P. Jaimes, P. Xia, K. R. Graham, M. L. Tang, T. Lian, *J. Am. Chem. Soc.* **2019**, *141*, 9769.

[32] E. Radiunas, M. Dapkevičius, S. Raišys, S. Juršėnas, A. Jozeliūnaitė, T. Javorskis, U. Šinkevičiūtė, E. Orentas, K. Kazlauskas, *Phys. Chem. Chem. Phys.* **2020**, *22*, 7392.

[33] L. Nienhaus, J.-P. Correa-Baena, S. Wieghold, M. Einzinger, T.-A. Lin, K. E. Shulenberger, N. D. Klein, M. Wu, V. Bulović, T. Buonassisi, M. A. Baldo, M. G. Bawendi, *ACS Energy Lett.* **2019**, *4*, 888.

[34] T. Ogawa, M. Hosoyamada, B. Yurash, T.-Q. Nguyen, N. Yanai, N. Kimizuka, *J. Am. Chem. Soc.* **2018**, *140*, 8788.

[35] S. Hoseinkhani, R. Tubino, F. Meinardi, A. Monguzzi, *Phys. Chem. Chem. Phys.* **2015**,*17*, 4020.

[36] N. Nishimura, V. Gray, J. R. Allardice, Z. Zhang, A. Pershin, D. Beljonne, A. Rao, *ACS Mater. Lett*. **2019**, *1*, *6*, 660.

[37] A. Monguzzi, J. Mezyk, F. Scotognella, R. Tubino, F. Meinardi, *Phys. Rev. B: Condens. Matter Mater. Phys.* **2008**, *78,* 195112.

[38] Y. Y. Cheng, T. Khoury, R. G. C. R. Clady, M. J. Tayebjee, N. J. Ekins-Daukes, M. J. Crossley, T. W. Schmidt, *Phys. Chem. Chem. Phys.* **2010**, *12*, 66.

[39] A. Haefele, J. Blumhoff, R. S. Khnayzer, F. N. Castellano, *J. Phys. Chem. Lett.* **2012**, *3*, 299.

[40] D. Y. Kondakov, T. D. Pawlik, T. K. Hatwar, J. P. Spindler, *J. Appl. Phys.* **2009**, *106,* 124510.

[41] N. Yanai, K. Suzuki, T. Ogawa, Y. Sasaki, N. Harada, N. Kimizuka, *J. Phys. Chem. A* **2019**, *123*, 10197.

[42] B. Valeur, *Molecular Fluorescence: Principles and Applications*, Wiley-VCH, Weinheim, **2002**.

[43] E. D. Gaspera, Y. Peng, Q. Hou, L. Spiccia, U. Bach, J. J. Jasieniak, Y.-B. Cheng, *Nano Energy* **2015**, *13*, 249.

[44] Z. Xu, Z. Liu, N. Li, G. Tang, G. Zheng, C. Zhu, Y. Chen, L. Wang, Y. Huang, L. Li, N. Zhou, J. Hong, Q. Chen, H. Zhou, *Adv. Mater.* **2019**, *31*, 1900390.

[45] R. C. Benson, H. A. Kues, *Phys. Med. Biol.* **1978**, *23*, 159.

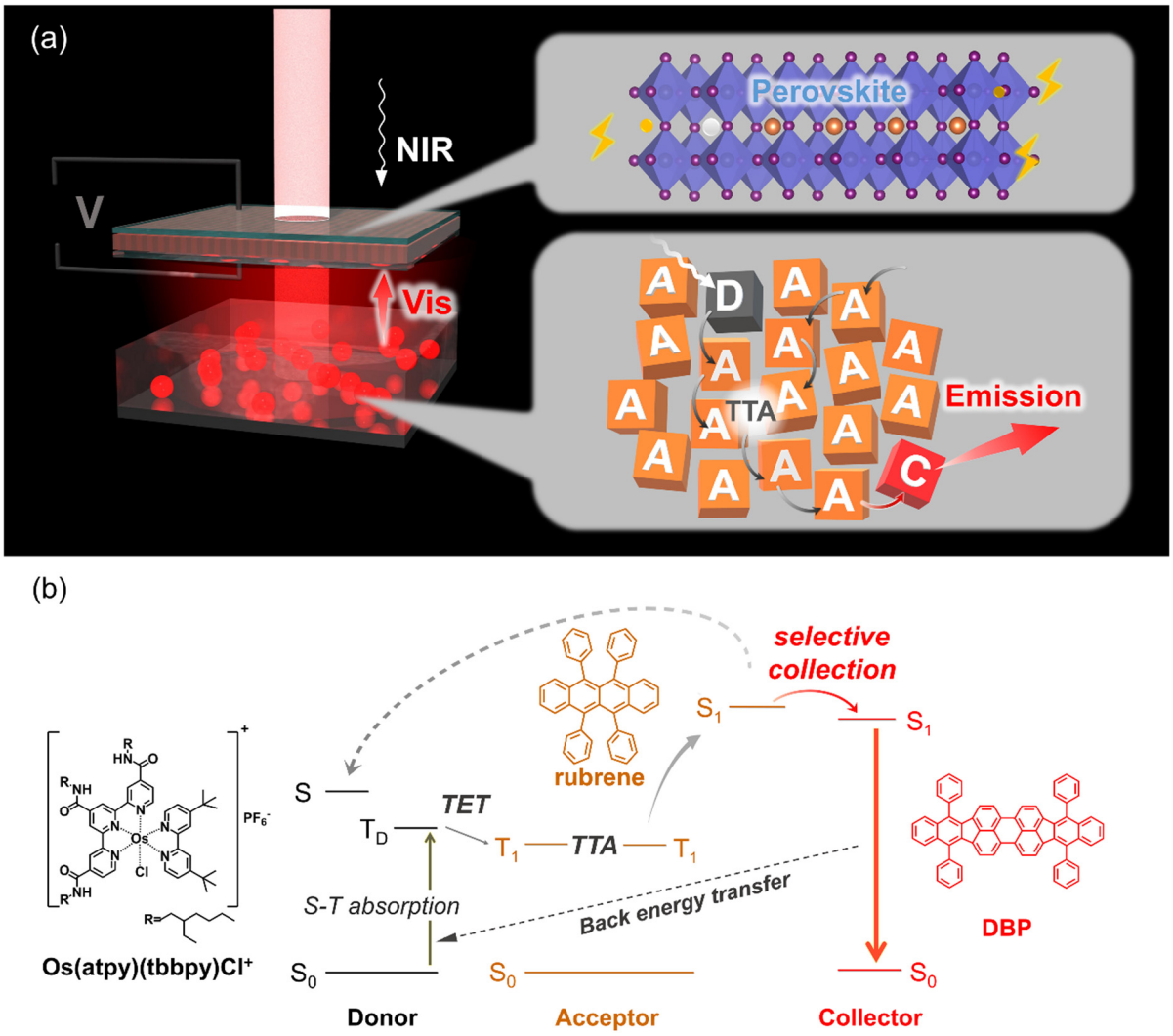

Figure 1. (a) Scheme of NIR-to-vis TTA-UC for photocurrent generation of perovskite solar cells. The upconverted emission is used for the excitation of perovskite solar cells. (b) Energy diagram for the TTA-UC system including S-T absorption and singlet energy collection. NIR light excitation of the S-T absorption donor leads to the donor-to-acceptor triplet energy transfer (TET), which is followed by triplet energy migration and TTA among acceptors. Resulting excited singlet energy again migrates among acceptor assemblies and is harvested to the highly fluorescent collector.

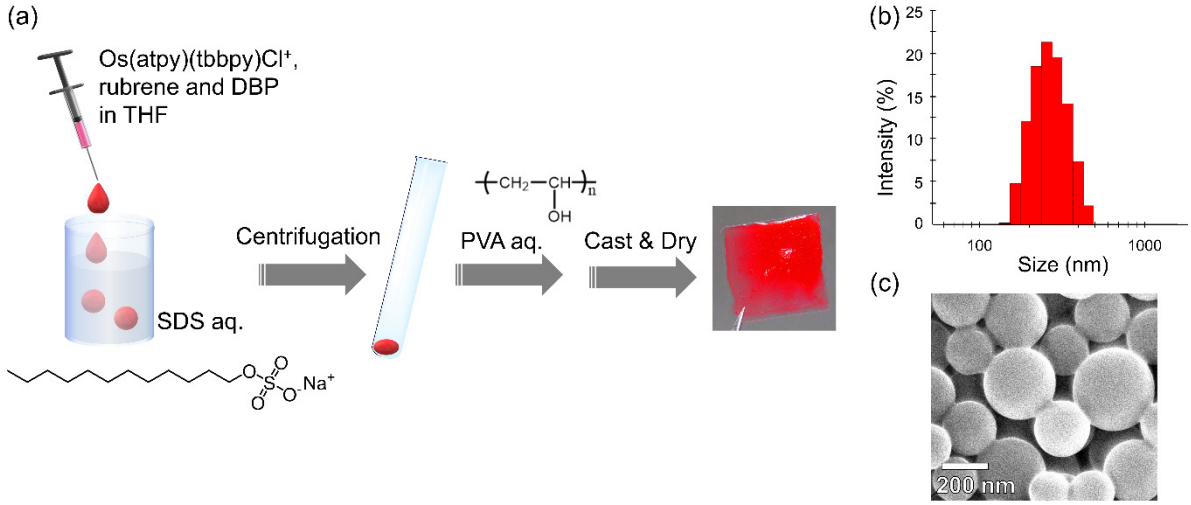

Figure 2. (a) Schematic representation for the preparation of donor/acceptor/collector ternary nanoparticles and their encapsulation into oxygen-blocking PVA films. (b) DLS profile of the Os(atpy)(tbbpy)Cl^+/rubrene/DBP nanoparticles dispersed in water. (c) SEM image of the Os(atpy)(tbbpy)Cl^+/rubrene/DBP nanoparticles.

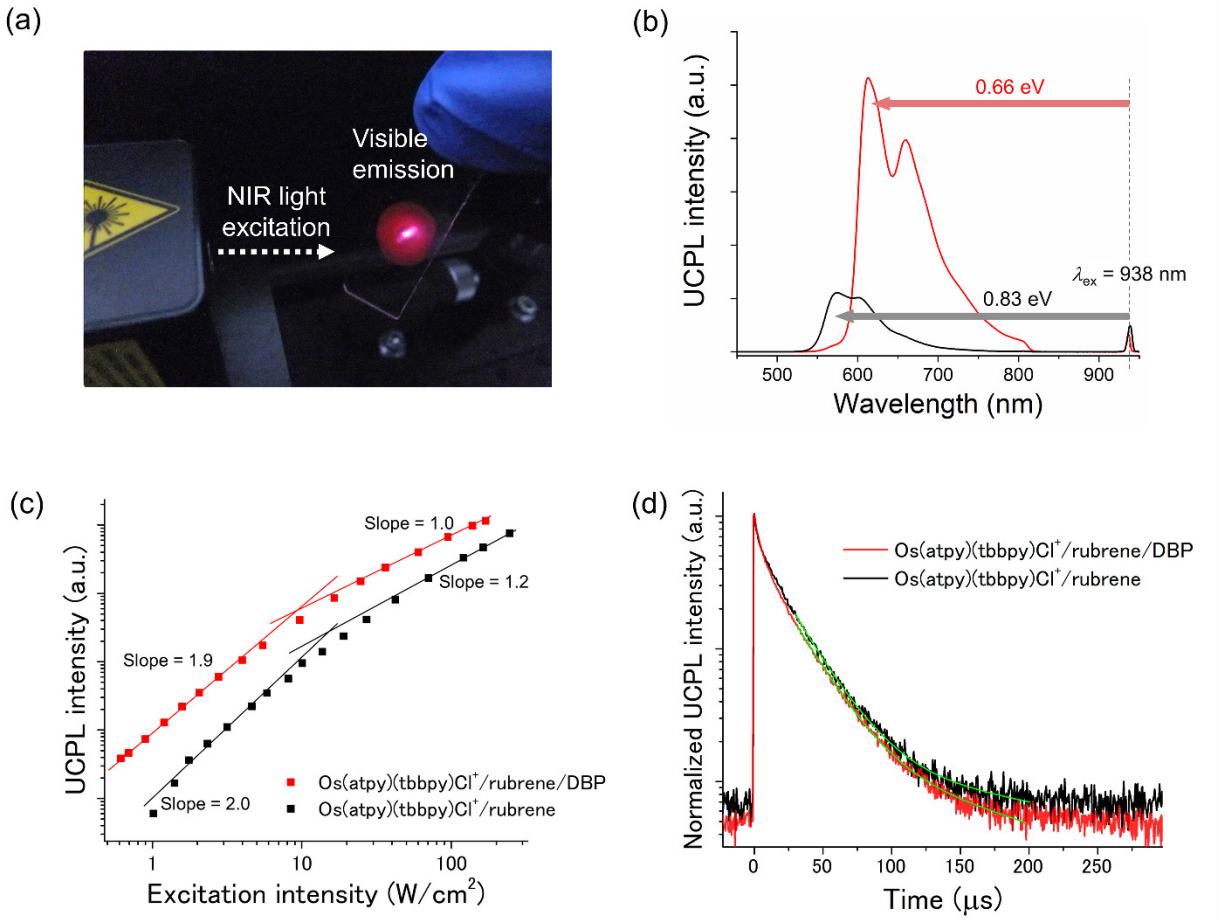

Figure 3. (a) Photograph of upconverted red emission of the Os(atpy)(tbbpy)Cl^+/rubrene/DBP film in air under 938 nm NIR excitation. (b) Upconverted emission spectra of the Os(atpy)(tbbpy)Cl^+/rubrene film (black) and the Os(atpy)(tbbpy)Cl^+/rubrene/DBP (red) film (λ_{ex} = 938 nm, 810 nm short pass filter). (c) Double-logarithmic plots of the UC emission intensity at 575 nm of the Os(atpy)(tbbpy)Cl^+/rubrene film (black) and at 625 nm of the Os(atpy)(tbbpy)Cl^+/rubrene/DBP (red) film as a function of excitation intensity of the 938 nm laser. The solid lines are fitting results with slopes of 1.9 or 2.0 and 1.1 or 1.2 in the low- and high-intensity regimes, respectively. (d) Time-resolved upconverted emission intensity at 575 nm of the Os(atpy)(tbbpy)Cl^+/rubrene film (black) and at 625 nm of the Os(atpy)(tbbpy)Cl^+/rubrene/DBP film (red) under pulsed excitation at 938 nm. The green fitting curves were obtained by considering the known relationship of $I_{UC}(t) \propto \exp(-2t/\tau_T)$, where τ_T is the acceptor triplet lifetime.

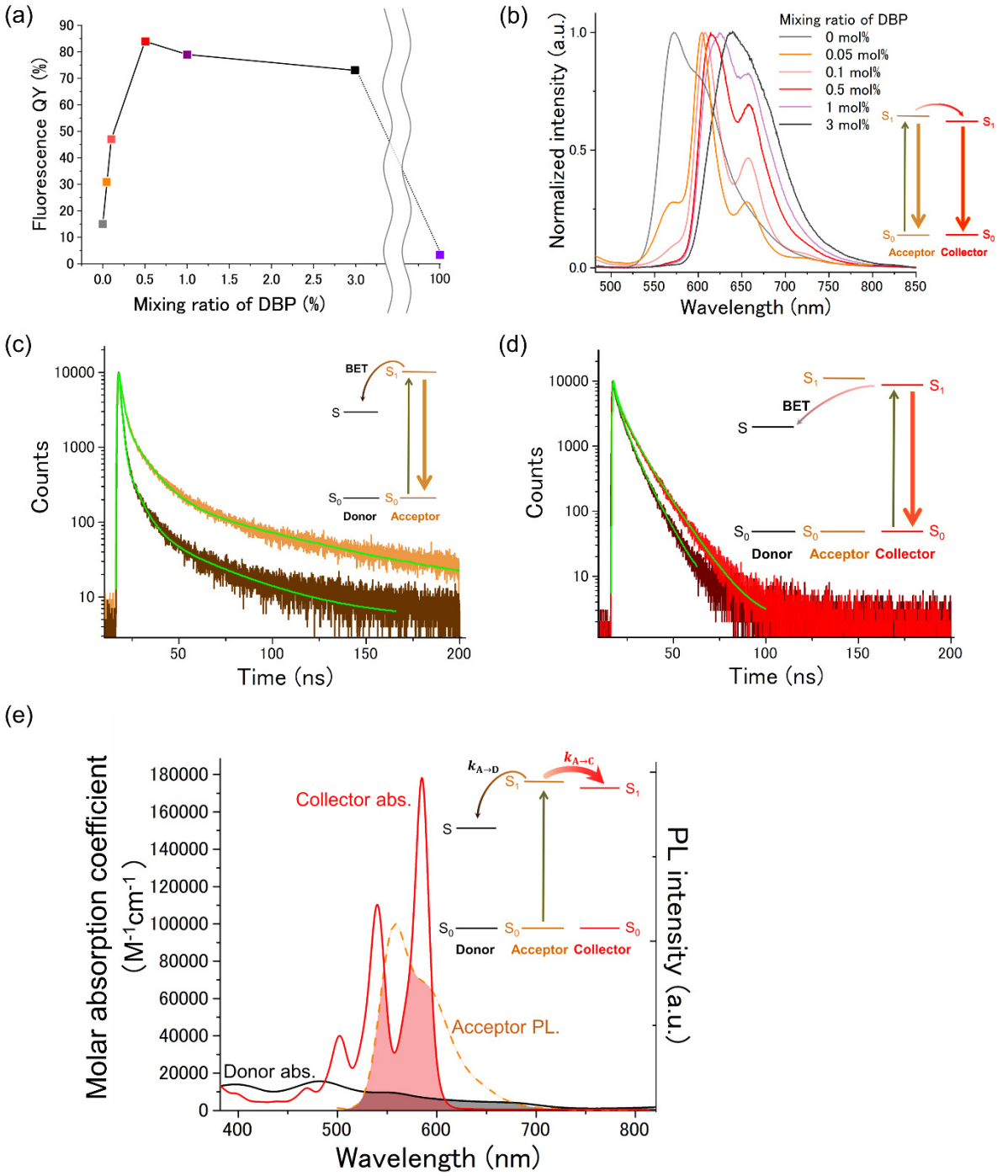

Figure 4. (a) Fluorescence quantum yield of rubrene/DBP films at various DBP contents (λ_{ex} = 462 nm). (b) Fluorescence spectra of rubrene/DBP films (λ_{ex} = 450 nm). (c) Fluorescence decays of the rubrene (orange) film and the Os(atpy)(tbbpy)Cl^{+}/rubrene (brown) film at 590 nm (λ_{ex} = 470 nm). Fitting curves are indicated by green lines. (d) Fluorescence decays of the rubrene/DBP (red) film and the Os(atpy)(tbbpy)Cl^{+}/rubrene/DBP (dark red) film at 640 nm (λ_{ex} = 470 nm). Fitting curves are indicated by green lines. (e) Spectral overlap between acceptor emission and donor/collector absorption.

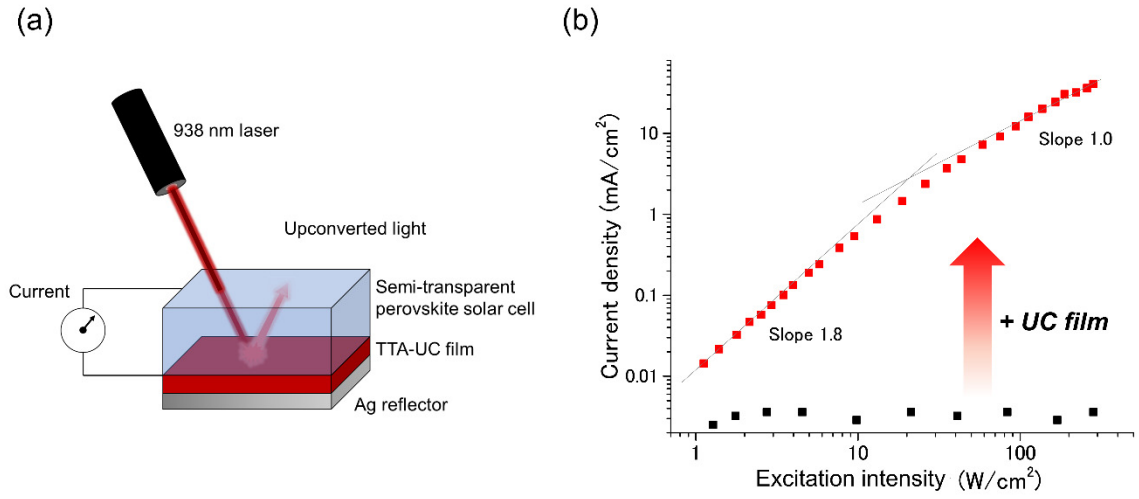

Figure 5. (a) Scheme of integrating the TTA-UC film at the rear side of the perovskite solar cell. Ag reflector helps to direct the upconverted emission back to the photovoltaic device. (b) Double-logarithmic plots of short-circuit photocurrent density with respect to excitation intensity (λ_{ex} = 938 nm).

Table of Content: Solid films showing an efficient NIR-to-vis photon upconversion based on triplet-triplet annihilation (TTA-UC) is achieved by the combined approaches of singlet-to-triplet (S-T) absorption and upconverted singlet energy harvesting to a highly fluorescent collector. The application of NIR-to-vis TTA-UC in photocurrent generation of perovskite solar cells is demonstrated for the first time.

Keyword: perovskite, solar cell, photon upconversion, triplet-triplet annihilation, energy collection

Mika Kinoshita, Yoichi Sasaki, Shogo Amemori, Naoyuki Harada, Zhanhao Hu, Zonghao Liu, Luis K. Ono, Yabing Qi,* Nobuhiro Yanai,* and Nobuo Kimizuka*

Title: Photon Upconverting Solid Films with Improved Efficiency for Endowing Near-Infrared Sensitivity to Perovskite Solar Cells